Optics & Laser Technology 47 (2013) 329–335

Contents lists available at SciVerse ScienceDirect

Optics & Laser Technology

journal homepage: www.elsevier.com/locate/optlastec

Review

# Biconjugate gradient stabilized method in image deconvolution of a wavefront coding system

Peng Liu [a], Qin-xiao Liu [a], Ting-yu Zhao [b], Yan-ping Chen [c], Fei-hong Yu [a,*]

[a] State Key Laboratory of Modern Optical Instrumentation, Optical Engineering Department, Zhejiang University, Hangzhou 310027, China
[b] Department of Physics, Zhejiang Sci-Tech University, Hangzhou 310018, China
[c] Physics Department, College of Science, Ningbo University of Technology, Ningbo 315211, China

ARTICLE INFO

*Article history:*
Received 8 January 2012
Received in revised form
18 August 2012
Accepted 21 August 2012
Available online 12 October 2012

*Keywords:*
Image deconvolution
Bi-CGSTAB
Wavefront coding system

ABSTRACT

The point spread function (PSF) is a non-rotational symmetric for the wavefront coding (WFC) system with a cubic phase mask (CPM). Antireflective boundary conditions (BCs) are used to eliminate the ringing effect on the border and vibration on the edge of the image. The Kronecker product approximation is used to reduce the computation consumption. The image-formation process of the WFC system is transformed into a matrix equation. In order to save storage space, biconjugate gradient (Bi-CG) and biconjugate gradient stabilized (Bi-CGSTAB) methods are used to solve the asymmetric matrix equation, which is a typical iteration algorithm of the Krylov subspace using the two-side Lanczos process. Simulation and experimental results illustrate the efficiency of the proposed algorithm for the image deconvolution. The result based on the Bi-CGSTAB method is smoother than the classic Wiener filter, while preserving more details than the Truncated Singular Value Decomposition (TSVD) method.

© 2012 Elsevier Ltd. All rights reserved.

**Contents**



## 1. Introduction

The image-formation process of the optical system is regarded as a convolution blurring process between the original image and the point spread function of the system.

$$G = h * X \tag{1-1}$$

where $X$ and $G$ are $n \times n$ matrices, denoting the object and the blurred image in the image plane respectively, $h$ is the point spread function (PSF) of the system and "$*$" denotes the convolution operator.

* Corresponding author.
*E-mail address:* feihong@zju.edu.cn (F.-h. Yu).

0030-3992/$ - see front matter © 2012 Elsevier Ltd. All rights reserved.
http://dx.doi.org/10.1016/j.optlastec.2012.08.022

The mathematical model can be described by the discrete linear equation

$$g = Hx \tag{1-2}$$

where the vector $x$ is formed by stacking the columns of $X$ into a single column vector, the $n^2 \times n^2$ matrix $H$ represents the blurring operator. In order to eliminate the ringing effect, $H$ is derived from the PSF by using the antireflective boundary conditions. In addition, the Kronecker product approximation is used to reduce the computation consumption. Then the image convolution blurring process can be expressed as a matrix equation [1–3].

Image deconvolution is the key for the WFC system to get the final sharp image, the difficulty lies in the ill-posed and asymmetric characteristic of the blurring operator. Truncated Singular Value Decomposition (TSVD) [3] is one of the common used methods to solve Eq. (1-2), but it abandons the small singular values, in this way some details of the image will be lost as noise and the deconvoluted image is not smooth. The classic Wiener filter is a fast method based on the Fast Fourier Transformation, but the ringing effect is very serious because the periodic boundary condition is used.

Conjugate gradient (CG) algorithm based on Lanczos orthogonalization procedure is a popular iterative method, but it is only suitable in solving the linear equation with positive definite coefficient matrix. In our wavefront coding system with the cubic phase mask [4–6], the PSF is non-rotational symmetric, and the image deconvolution can be modeled as a large-scale asymmetric linear discrete problem. We first present Bi-CG and Bi-CGSTAB methods based on the two-side Lanczos tridiagonalization algorithm to find the smooth deconvoluted solution without ringing effect which stands for the final sharp image. Two-side Lanczos tridiagonalization algorithm is a polynomial algorithm, which takes less storage than the Arnoldi algorithm [7,8].

The paper is organized as follows: Section 2 gives the new blurring model which combines the antireflective BCs and the Kronecker product approximation. Section 3 reviews the two-side Lanczos tridiagonalization algorithm and presents the Bi-CG and Bi-CGSTAB methods. The modified Bi-CG and Bi-CGSTAB algorithms are presented to solve the asymmetric matrix equation in Section 4. Simulation and experimental results are given in Section 5.

## 2. Image convolution blurring model

### 2.1. Antireflective boundary conditions

The structure of the convolution blurring operator $H$ depends on the boundary conditions. In recent years antireflective boundary conditions are found to be effective to describe the real convolution of the image border.

Antireflective BCs reflect the image with respect to the boundaries by using a central symmetry. This procedure preserves the $C^1$ continuity of the image, and the ringing effects are negligible. Antireflective BCs lead to a block structure of the PSF matrices that can be described as block Toeplitz-plus-Hankel-plus-Hankel-plus-Rank-2 with Toplitz-plus-Hankel-plus-Rank-2 block (BTHR2THR2B) [9–11].

### 2.2. Kronecker product

Let $A \in C^{m\times n}$ and $B \in C^{p\times q}$ be two matrices, and $(A)_{ij}=a_{ij}$, the Kronecker product $D = A \otimes B \in C^{mp\times nq}$ is defined by

$$D = A \otimes B = \begin{pmatrix} a_{11}B & a_{12}B & \cdots & a_{1n}B \\ a_{21}B & a_{22}B & \cdots & a_{2n}B \\ \vdots & & \ddots & \vdots \\ a_{m1}B & a_{m2}B & \cdots & a_{mb}B \end{pmatrix} \tag{2-1}$$

The Kronecker product has the following property:

$$A_1XA_2^T = B \Leftrightarrow (A_2 \otimes A_1)\mathrm{vec}(X) = \mathrm{vec}(B) \tag{2-2}$$

Taking advantage of this relationship, the two blurring matrices $A_1$ and $A_2$ can be written in the normal form as

$$A_1XA_2^T = B \Leftrightarrow (A_2 \otimes A_1)\mathrm{vec}(X) = \mathrm{vec}(B) \Rightarrow Ax = b \tag{2-3}$$

where $A_1 \otimes A_2 = A \in R^{mn\times mn}$, $x,b \in R^{mn}$, $\mathrm{vec}(X)$ is formed by stacking the columns of $X$ into a single column vector ($\mathrm{vec}(X)=x$).

A general idea to decompose the convolution operator is to find matrices $A_k$ and $B_k$ ($k = 1,2,\ldots,s$) which fulfill

$$\min \|H - \sum_{k=1}^{s} (A_k \otimes B_k)\|_F \tag{2-4}$$

where $\|\bullet\|_F$ represents the Frobenius norm [1–3]. Then the convolution blurring model can be described as

$$G = H_1XH_2^T \tag{2-5}$$

where $G$ is the observed image, $H_1$ and $H_2$ represent the two blurring matrices, and $X$ is the true image we need.

## 3. Two-side Lanczos tridiagonalization algorithm

The two-side Lanczos tridiagonalization algorithm [12] chooses the bases $(v^{(1)},v^{(2)},\ldots,v^{(m)})$, $(\omega^{(1)},\omega^{(2)},\cdots,\omega^{(m)})$ from the Krylov subspaces $\Re_m(A,v^{(1)})$ and $\Re_m(A^T,\omega^{(1)})$, respectively. We define the inner product $(A,B)=\mathrm{trace}(A^TB)$, where $\mathrm{trace}(\bullet)$ denotes the trace and $A^T$ is the transpose of the matrix $A$. The algorithm can be summarized as follows:

**Algorithm 1.** Two-side Lanczos tridiagonalization algorithm

Step 1: Choose vector $v^{(1)}$ and $\omega^{(1)}$, $(v^{(1)},\omega^{(1)})=1$, set $\theta_1=\gamma_1=0$, $\omega^{(0)}=v^{(0)}=0$, $j=1$.

Step 2: Compute the parameter $\delta_j=(Av^{(j)},\omega^{(j)})$.

Step 3: Compute $\overline{v}^{(j+1)} = Av^{(j)} - \delta_j v^{(j)} - \theta_j v^{(j-1)}$, $\overline{\omega}^{(j+1)} = A^T\omega^{(j)} - \delta_j\omega^{(j)} - \gamma_j v^{(j-1)}$.

Step 4: Compute $\gamma_{j+1} = \left|(\overline{v}^{(j+1)},\overline{\omega}^{(j+1)})\right|^{1/2}$, if $\gamma_{j+1}=0$, stop.

Step 5: Compute $\theta_{j+1} = (\overline{v}^{(j+1)},\overline{\omega}^{(j+1)})/\gamma_{j+1}$, $\omega^{(j+1)} = \overline{\omega}^{(j+1)}/\theta_{j+1}$, and $v^{(j+1)} = \overline{v}^{(j+1)}/\gamma_{j+1}$. If $j<m$, set $j=j+1$, go to Step 2.

This algorithm constructs an asymmetric tridiagonal matrix:

$$T_m = \begin{bmatrix} \delta_1 & \theta_2 & & & \\ \gamma_2 & \delta_2 & \theta_3 & & \\ & \ddots & \ddots & \ddots & \\ & & \gamma_{m-1} & \delta_{m-1} & \theta_m \\ & & & \gamma_m & \delta_m \end{bmatrix} \tag{3-1}$$

It is easy to find that

$$(v^{(i)},\omega^{(j)}) = \begin{cases} 1, & i=j \\ 0, & i\neq j \end{cases}. \quad (v^{(1)},v^{(2)},\ldots,v^{(m)}) \quad \text{and} \quad (\omega^{(1)},\omega^{(2)},\ldots,\omega^{(m)})$$

are the bases of the Krylov subspaces $\Re_m(A^T,v^{(1)})$ and $\Re_m(A^T,\omega^{(1)})$, respectively. In addition,

$$AV_m = V_mT_m + \gamma_{m+1}v^{(m+1)}(e^{(m)})^T \tag{3-2}$$

$$A^TV_m = W_mT_m + \theta_{m+1}\omega^{(m+1)}(e^{(m)})^T \tag{3-3}$$

$$W_m^TAV_m = T_m \tag{3-4}$$

where $V_m=[v^{(1)},v^{(2)},\ldots,v^{(m)}]$, $W_m=[\omega^{(1)},\omega^{(2)},\ldots,\omega^{(m)}]$, and $e^{(m)}$ is the unit vector with the $m$th element equal to 1.

The two-side Lanczos algorithm takes less storage than the Arnoldi algorithm because it only needs to store six vectors every iteration. The computation consumption becomes much less than the Arnoldi algorithm along with the increase of $m$.

### 3.1. Bi-CG method

In order to solve the equations $Ax=b$ and $A^Tx_t=b_t$, we choose $v^{(1)}=r^{(0)}=b-Ax^{(0)}$, $\omega^{(1)}=r_t^{(0)}=b_t-Ax_t^{(0)}$. Then we define $x^{(m)}$ and $r^{(m)}$ as the approximate solution and residua of equation $Ax=b$. Similarly, $x_t^{(m)}$ and $r_t^{(m)}$ represent the approximate solution and residua of equation $A^Tx_t=b_t$.

The Bi-CG method can be summarized as follows:

**Algorithm 2.** The Bi-CG method for asymmetric linear equation

Step 1: Compute $r^{(0)}=b-Ax^{(0)}$, choose$r_t^{(0)}$ and $(r^{(0)},r_t^{(0)})\neq 0$, set $s^{(0)}=r^{(0)},s_t^{(0)}=r_t^{(0)}$, $j=0$.
Step 2: Compute the parameter $\alpha_j=(r^{(j)},r_t^{(j)})/(As^{(j)},s_t^{(j)})$.
Step 3: Compute $x^{(j+1)}=x^{(j)}+\alpha_j s^{(j)},r^{(j+1)}=r^{(j)}-\alpha_j As^{(j)},r_t^{(j+1)}=r_t^{(j)}-\alpha_j A^Ts_t^{(j)}$, if $x^{(j+1)}$ achieves the accuracy, stop.
Step 4: Compute $\beta_j=(r^{(j+1)},r_t^{(j+1)})/(r^{(j)},r_t^{(j)}),s^{(j+1)}=r^{(j+1)}+\beta_j s^{(j)}$, $s_t^{(j+1)}=r_t^{(j+1)}+\beta_j s_t^{(j)}$, set $j=j+1$, go to Step 2.

### 3.2. Bi-CGSTAB method

In the Bi-CG method, the product between $A^T$ and other vectors has to be computed and stored. In order to avoid this operation, the recursive polynomial technology is introduced. The residual vector and the direction vector can be put into the following expression:

$$r^{(j)}=\phi_{(j)}(A)r^{(0)}\quad r_t^{(j)}=\phi_j(A^T)r_t^{(0)}\quad s^{(j)}=\pi_j(A)r^{(0)},\quad s_t^{(j)}=\pi_j(A^T)r_t^{(0)}$$
$$\phi_{j+1}(\varepsilon)=\phi_j(\varepsilon)-\alpha_j\varepsilon\pi_j(\lambda),\pi_{j+1}(\varepsilon)=\phi_{j+1}(\lambda)+\beta_j\pi_j(\lambda) \quad (3-5)$$

where $\phi_j$ and $\pi_j$ are polynomials of degree $j$ and $\phi_j(0)=1$.

The Bi-CGSTAB method is a multiplication Lanczos method, which defines the residua as follows:

$$r_{STA}^{(j)}=\psi_j(A)\phi_j(A)r^{(0)},\quad p^{(j)}=\psi_j(A)\pi_j(A)r^{(0)} \quad (3-6)$$

$$\psi_0(\varepsilon)=1,\quad \psi_{j+1}(\varepsilon)=(1-\mu_j\varepsilon)\psi_0(\varepsilon) \quad (3-7)$$

where $\mu_j$ is the undetermined coefficient;

$$r_{STA}^{(j+1)}=(1-\mu_jA)(r_{STA}^{(j)}-\alpha_jAp^{(j)}),p^{(j+1)}=r_{STA}^{(j+1)}+\beta_j(p^{(j)}-\mu_jAp^{(j)}) \quad (3-8)$$

Consider an arbitrary $q_i(\varepsilon)(i<j)$, as $q_i(A^T)r_t^{(0)}\in\Re_{i+1}(A^T,r_t^{(0)})\subset\Re_j(A^T,r_t^{(0)})$ and $r_{BICG}^{(j)}=b-Ax_{BICG}^{(j)}\perp\Re_j(A^T,r_t^{(0)})$, where subscript *BICG* corresponds to the vectors of the Bi-CG method. So it can be found that $(\phi_j(A)r^{(0)},q_i(A^T)r_t^{(0)})=0$.

As the leading coefficient of $\phi_j$ is equal to the one of $\pi_j$,

$$\alpha_j=\frac{(\phi_j(A)r^{(0)},\phi_j(A^T)r_t^{(0)})}{(A\pi_j(A)r^{(0)},\pi_j(A^T)r_t^{(0)})}=\frac{(\phi_j(A)r^{(0)},\pi_j(A^T)r_t^{(0)})}{(A\pi_j(A)r^{(0)},\pi_j(A^T)r_t^{(0)})}$$
$$=\frac{(\phi_j(A)r^{(0)},\psi_j(A^T)r_t^{(0)})}{(A\pi_j(A)r^{(0)},\psi_j(A^T)r_t^{(0)})}=\frac{(r_{STA}^{(j)},r_t^{(0)})}{(Ap^{(j)},r_t^{(0)})} \quad (3-9)$$

Consider Eqs. (3-5) and (3-7), the leading coefficient of $\phi_j(\lambda)$ and $\psi_j(\lambda)$ are $(-1)^j\alpha_{j-1},\cdots,\alpha_0$, and $(-1)^j\mu_{j-1},\cdots,\mu_0$, respectively:

$$\beta_j=\frac{(\phi_{j+1}(A)r^{(0)},\phi_{j+1}(A^T)r_t^{(0)})}{(\phi_j(A)r^{(0)},\phi_j(A^T)r_t^{(0)})}=\frac{(\phi_{j+1}(A)r^{(0)},\psi_{j+1}(A^T)r_t^{(0)})\alpha_j}{(\phi_j(A)r^{(0)},\psi_j(A^T)r_t^{(0)})\mu_j}=\frac{(r_{STA}^{(j+1)},r_t^{(0)})}{(r_{STA}^{(j)},r_t^{(0)})}\frac{\alpha_j}{\mu_j} \quad (3-10)$$

In order to minimize $\|r_{STA}^{(j+1)}\|_2$ as low as possible, $\mu_j$ is selected as follows:

$$\mu_j=\frac{(Aq^{(j)},q^{(j)})}{(Aq^{(j)},Aq^{(j)})} \quad (3-11)$$

where $q^{(j)}=r_{STA}^{(j)}-\alpha_jAp^{(j)}$. Then the following recursive relationship is obtained:

$$r_{STA}^{(j+1)}=q^{(j)}-\mu_jAq^{(j)}=r_{STA}^{(j)}-\alpha_jAp^{(j)}-\mu_jAq^{(j)} \quad (3-12)$$

$$x^{(j+1)}=x^{(j)}+\alpha_jp^{(j)}+\mu_jq^{(j)} \quad (3-13)$$

The above Bi-CGSTAB method can be summarized as follows:

**Algorithm 3.** The Bi-CGSTAB method

Step 1: Compute $r_{STA}^{(0)}=b-Ax^{(0)}$, choose an arbitrary matrix $r_t^{(0)}$, set $p^{(0)}=r_{STA}^{(0)}$, $j=0$.
Step 2: Compute $\alpha_j=(r_{STA}^{(j)},r_t^{(0)})/(Ap^{(j)},r_t^{(0)}),q^{(j)}=r_{STA}^{(j)}-\alpha_jAp^{(j)}$.
Step 3: Compute $\mu_j=(Aq^{(j)},q^{(j)})/(Aq^{(j)},Aq^{(j)})$.
Step 4: Compute $x^{(j+1)}=x^{(j)}+\alpha_jp^{(j)}+\mu_jq^{(j)}$, and $r_{STA}^{(j+1)}=q^{(j)}-\mu_jAq^{(j)}$. if $x^{(j+1)}$ achieves the accuracy, stop.
Step 5: Compute $\beta_j=((r_{STA}^{(j+1)},r_t^{(0)})/(r_{STA}^{(j)},r_t^{(0)}))(\alpha_j/\mu_j)$.
Step 6: Compute $p^{(j+1)}=r_{STA}^{(j+1)}+\beta_j(p^{(j)}-\mu_jAp^{(j)})$, $j=j+1$, go to Step 2.

## 4. Image deconvolution algorithm using the Bi-CG and Bi-CGSTAB methods

In order to deconvolute the blurred image with the Bi-CG method, the following modified version is given by considering the convolution blurring model described in Eq. (2-5).

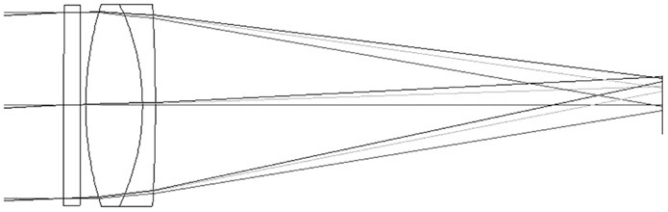

**Fig. 1.** The simple doublet lens system with the cubic phase mask.

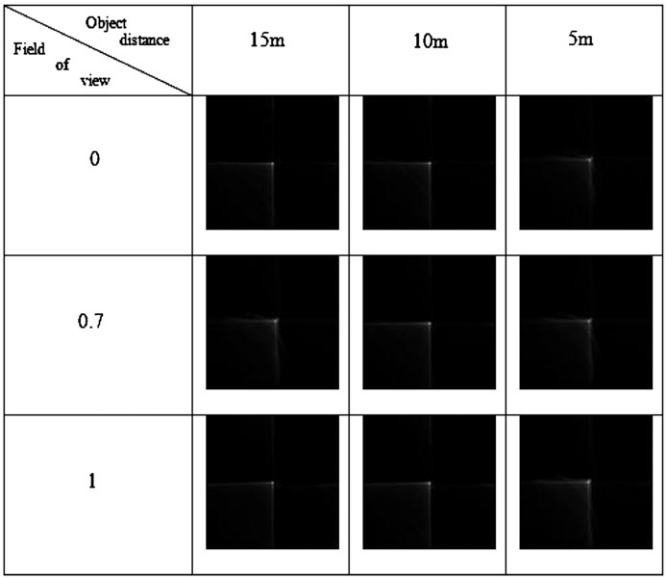


**Fig. 2.** The PSF of the simple double lens system with the cubic phase mask for object distance 15 m, 10 m and 5 m.

**Algorithm 4.** Modified Bi-CG method for image deconvolution

Step 1: Choose $X^{(0)}$, compute $r_{STA}^{(0)}=G-H_1X^{(0)}H_2^T$, choose $r_t^{(0)}$ and $(r_{STA}^{(0)},r_t^{(0)})\neq 0$, set $s^{(0)}=r^{(0)},s_t^{(0)}=r_t^{(0)},j=0$.
Step 2: Compute the parameter $\alpha_j=(r^{(j)},r_t^{(j)})/(H_1s^{(j)}H_2^T,s_t^{(j)})$.
Step 3: Compute $x^{(j+1)}=x^{(j)}+\alpha_js^{(j)},r_{STA}^{(j+1)}=r_{STA}^{(j)}-\alpha_jH_1s^{(j)}H_2^T$, $r_t^{(j+1)}=r_t^{(j)}-\alpha_jH_1^Ts_t^{(j)}H_2$, if $x^{(j+1)}$ achieves the accuracy, stop.
Step 4: Compute $\beta_j=(r_{STA}^{(j+1)},r_t^{(j+1)})/(r_{STA}^{(j)},r_t^{(j)}),s^{(j+1)}=r^{(j+1)}+\beta_js^{(j)},s_t^{(j+1)}=r_t^{(j+1)}+\beta_js_t^{(j)}$, set $j=j+1$, go to Step 2.

Similarly, we can give the modified version based on the Bi-CGSTAB method for image deconvolution by considering the convolution blurring model.

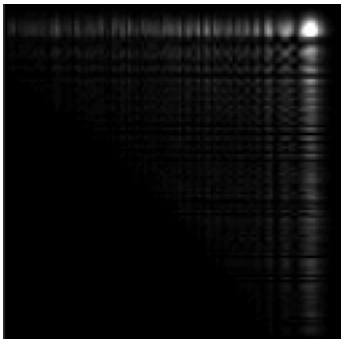

**Fig. 3.** The PSF used for restoration.

**Algorithm 5.** Modified Bi-CGSTAB method for image deconvolution

Step 1: Choose $X^{(0)}$, compute $r_{STA}^{(0)}=G-H_1X^{(0)}H_2^T$, choose an arbitrary matrix $r_t^{(0)}$, set $p^{(0)}=r_{STA}^{(0)},j=0$.
Step 2: Compute $\alpha_j=(r_{STA}^{(j)},r_t^{(0)})/(H_1p^{(j)}H_2^T,r_t^{(0)}),q^{(j)}=r_{STA}^{(j)}-\alpha_jH_1p^{(j)}H_2^T$.
Step 3: Compute $\mu_j=(H_1q^{(j)}H_2^T,q^{(j)})/(H_1q^{(j)}H_2^T,H_1q^{(j)}H_2^T)$,
Step 4: Compute $X^{(j+1)}=X^{(j)}+\alpha_jp^{(j)}+\mu_jq^{(j)}$, and $r_{STA}^{(j+1)}=q^{(j)}-\mu_jH_1q^{(j)}H_2^T$. if $X^{(j+1)}$ achieves the accuracy, stop.
Step 5: Compute $\beta_j=((r_{STA}^{(j+1)},r_t^{(0)})/(r_{STA}^{(j)},r_t^{(0)}))(\alpha_j/\mu_j)$.
Step 6: Compute $p^{(j+1)}=r_{STA}^{(j+1)}+\beta_j(p^{(j)}-\mu_jH_1p^{(j)}H_2^T)$, $j=j+1$, go to Step 2.

Here we introduce the relative error $\|\hat{X}-X^{(k)}\|_2/\|X^{(k)}\|_2$, where $\hat{X}$ is the original image, $X^{(k)}$ stands for the $k$th restoration image. The acceptable restored image is determined by the minimal relative error.

## 5. Simulation and experimental results

In this section, simulation and experimental results are given based on the Bi-CG and Bi-CGSTAB methods discussed above in a real wavefront coding system with the cubic phase mask. The blurring image $G$ is chosen as the initial $X^{(0)}$ and unit matrix as $r_t^{(0)}$. Finally, the solution is obtained which represents the true image needed. The results of the classic Wiener filter and the TSVD method is presented as the contrast.

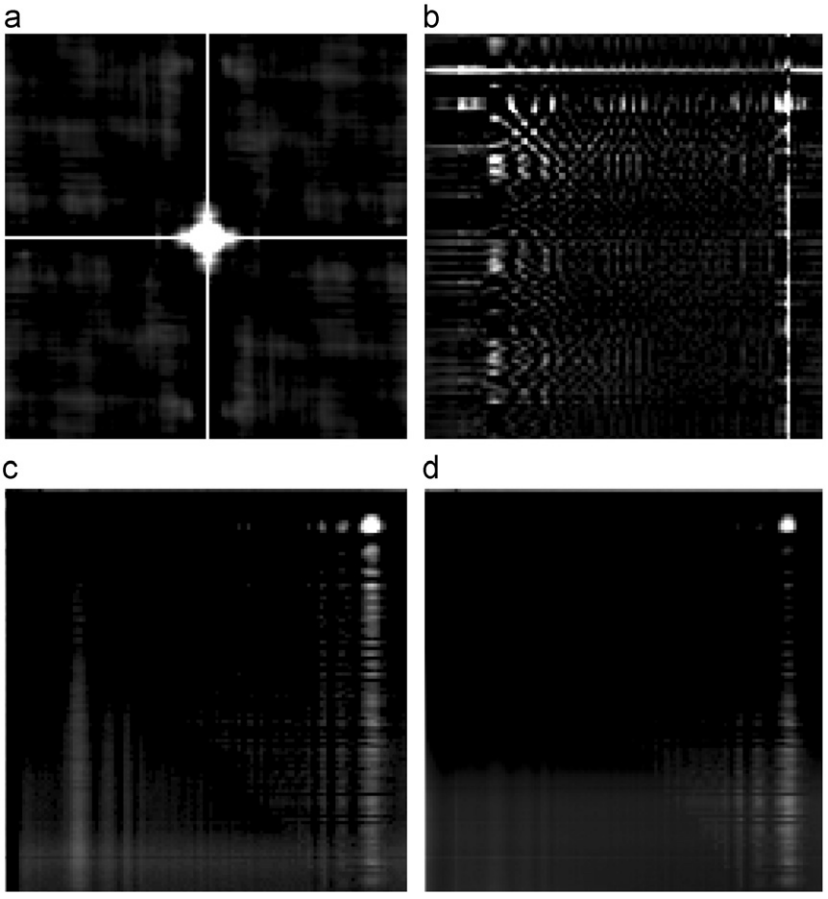


**Fig. 4.** The reconstructed points by the classic Wiener filter (a), TSVD method (b), Bi-CG (c) and Bi-CGSTAB method (d).

### 5.1. Simulation results

Fig. 1 gives the layout of our wavefront coding system with the cubic phase mask. It is a simple doublet lens with the optimal CPM on the pupil plane. Its focal length is 100 mm and $F$ number is 3. Its phase function is normalized as $Z=\alpha(X^3+Y^3)(a=1.2\times10^{-5})$.

Fig. 2 gives the different field's PSF of this system for object distance of 15 m, 10 m and 5 m. It can be found that the PSF has same pattern (right angled triangle) for object distance of 15 m, 10 m and 5 m for the deconvolution simulation. It is possible to use one PSF to restore the blurred image. Here the PSF of 0 field and 15 m is used for the restoration and the detail can found in Fig. 3. First we manipulate it with antireflective boundary conditions and the Kronecker product, and then new blurring model

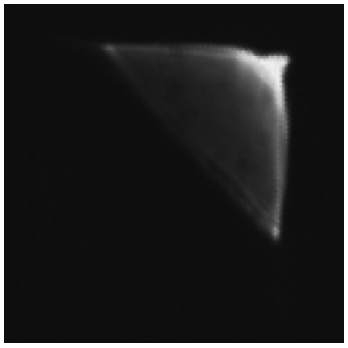

**Fig. 6.** The point spread function of the real WFC system.

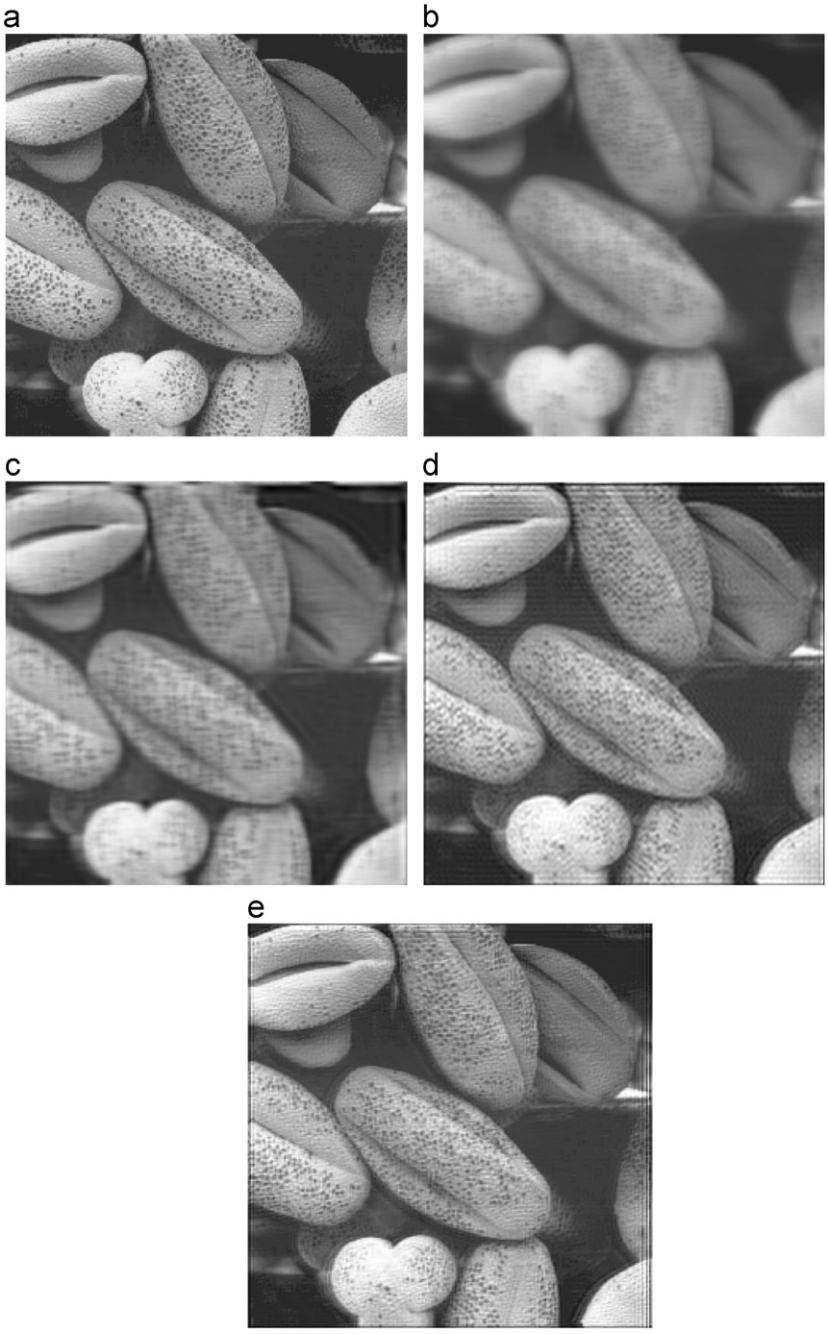


**Fig. 5.** (a) Original image, (b) blurred image, (c) deconvoluted image based on the Wiener filter, (d) deconvoluted image based on the TSVD method, and (e) deconvoluted image based on the Bi-CGSTAB method.


**Fig. 7.** (a) Real intermediate blurred image, (b) deconvoluted image based on the Wiener filter, (c) deconvoluted image based on the TSVD method, and (d) deconvoluted image based on the Bi-CGSTAB method.

matrix is acquired. Second the Bi-CGSTAB method is implemented to deconvolute the blurring model equation. Then the deconvoluted image is obtained.

Fig. 4 presents the reconstructed points, which are the numerical results of the PSF deconvoluted by itself. We give the results based on the Wiener filter, TSVD method and two-side Lanczos tridiagonalization algorithm, the reconstructed point of the classic Wiener filter is a big cross. TSVD, Bi-CG and Bi-CGSTAB methods give similar results, but the TSVD method has more oscillation, which will lead to lots of artificial stripes. Bi-CG and Bi-CGSTAB methods give smooth deconvoluted results, but the point given by the Bi-CGSTAB method is smaller than that of the Bi-CG. It demonstrates that the Bi-CGSTAB algorithm is an effective deconvolution method.

Fig. 5 gives the results of image deconvolution based on the classic Wiener filter TSVD, Bi-CG and Bi-CGSTAB methods. Fig. 5(a) is the original image; Fig. 5(b) is the blurred image, Fig. 5(c) is the acquired result deconvoluted by the classic Wiener filter. Fig. 5(d) is the deconvoluted image based on the TSVD method and Fig. 5(e) is the results based on the Bi-CGSTAB method.

It can be found that the modified Bi-CGSTAB method and the TSVD method both can give more excellent deconvolution result than the classic Wiener filter. But the result based on the TSVD method has more vibrations and the modified Bi-CGSTAB method preserves more details of the image than the TSVD method.

### 5.2. Experimental results

Fig. 6 shows the point spread function of the real WFC system with the cubic phase mask. The PSF is non-rotation symmetric and nearly insensitive for the object distance from 15 m to 5 m.

The real intermediate blurred image is shown in Fig. 7(a). It is acquired from the real doublet WFC system with the CPM. The CCD is IPX-1M48C of the IMPERX Corporation, whose active pixel resolution is $1000 \times 1000$ with the pixel size of $7.4\ \mu m \times 7.4\ \mu m$ and the S/N ratio is 55 dB. In the hallway illuminated by the incandescent lamp, three boys stand at distances of 15 m, 10 m and 5 m. The camera is set to automatic exposure. Their images are all encoded by the WFC system. The aim is to deconvolute this image and get the real scene for all of them as our eyes see.

Fig. 7(b) is the result of the image deconvolution based on classic Wiener filter. It has obvious ringing effect and vibration on the edge. Fig. 7(c) shows the deconvoluted result by the TSVD method, it introduces the cross stripes and morphs the image. Fig. 7(d) is the result based on the Bi-CGSTAB method with antireflective BCs. This method gives the smooth deconvoluted result. Fig. 7 indicates that the Bi-CGSTAB method is more effective than the Wiener filter and TSVD. There is little ringing effect on the image border and little vibration on the edge, and more details has been preserved.

## 6. Conclusion

In this paper a novel convolution blurring model is presented for the wavefront coding system with a cubic phase mask by combining the antireflection boundary conditions and the Kronecker product. The Bi-CGSTAB method is used in the image deconvolution for the new convolution equation. Simulation and experimental results show that the proposed method can give smooth deconvoluted image without ringing effect on the border and vibration on the edge of the image. It is proved to be a more effective deconvolution method for the non-rotational symmetric PSF than the classic Wiener filter and the TSVD method.

## Acknowledgment

This project is supported by the Chinese National Natural Science Foundation under the Contract 60777002 and the Ningbo Science and Technology Bureau under the Contract number 2008A610035.

## References

[1] Kamm J, Nagy JG. Optimal Kronecker product approximation of block Toeplitz matrices. SIAM Journal on Matrix Analysis and Applications 2000;22(1): 155–72.

[2] Kilmer ME, Nagy JG. Kronecker product approximations for dense block Toeplitz–plus–Hankel matrices. Numerical Linear Algebra with Applications 2007;14:581–602.

[3] Perrone L. Kronecker product approximations for image restoration with anti-reflective boundary conditions. Numerical Linear Algebra with Applications 2006;13:1–22.

[4] Dowski Jr. ER, Cathey WT. Extended depth of field through wavefront coding. Applied Optics 1995;34(11):1859–66.

[5] Zhao TY, Ye Z, Zhang WZ, Chen YP, Yu FH. Wide viewing angle skewed effect of the point spread function in a wavefront coding system. Optics Letters 2007;32(10):1220–2.

[6] Zhang WZ, Ye Z, Zhao TY, Chen YP, Yu FH. Point spread function characteristics analysis of the wavefront coding system. Optics Express 2007;15(4):1543–52.

[7] Sonneveld P. CGS: a fast Lanczos-type solver for nonsymmetric linear system. SIAM Journal on Scientific and Statistical Computing 1989;10:36–52.

[8] van der Vorst HA. Bi-CGSTAB: a fast and smoothly converging variant of Bi-CG for the solution of non-symmetric linera systems. SIAM Journal on Scientific and Statistical Computing 1992;12:631–44.

[9] Serra-Capizzano S. A note on antireflective boundary conditions and fast deblurring models. SIAM Journal on Scientific Computing 2003;25(4):1307–25.

[10] Christiansen M, Hanke M. Deblurring methods using antireflective boundary conditons. SIAM Journal on Scientific Computing 2007;30(2):855–72.

[11] Donatelli M, Estatico C, Martinelli A, Serra-Capizzano S. Improved image deblurring with anti-reflective boundary conditions and re-blurring. Inverse Problems 2006;22:2035–53.

[12] Cullum J, Zhang T. Two-sided Arnoldi and nonsymmetric Lanczos algorithm. SIAM Journal on Matrix Analysis and Applications 2002;24(2):303–19.